

# Permeation of Simple Gases Through Plasma Polymerized Films from Fluorine-Containing Monomers

SAEJOONG OH, YUAN ZENG, JA-KYUNG KOO, and W. P. ZURAWSKY\*

Department of Chemical Engineering, Polytechnic University, 333 Jay Street, Brooklyn, New York 11201

## SYNOPSIS

The permeation of several different permanent gases through plasma polymer membranes was studied. The plasma polymers were produced by a microwave discharge of various fluorine-containing monomers. Plasma polymers made from fluorine-rich monomers ( $F/C \approx 1$ ) yield films with the highest selectivities; those made from low fluorine content monomers show very little selectivity among the various gases.  $CO_2$  solubility is very high in the fluorine-rich plasma polymers and gives rise to large  $CO_2$  to  $CH_4$  selectivities. © 1995 John Wiley & Sons, Inc.

## INTRODUCTION

The permeability coefficients and ideal selectivities of plasma polymerized thin films have been examined by a number of different groups.<sup>1-9</sup> In most cases the selectivity of the plasma films to oxygen over nitrogen has been tested; the permeation of other gases through plasma polymer films has been examined in only a few cases. Oxygen to nitrogen selectivities of about 4 are not uncommon with plasma polymer films and values up to 7.2 have been reported for films made from perfluorobenzene/ $CF_4$  mixtures.<sup>4</sup>

For plasma polymers, the highest oxygen to nitrogen selectivity results that have been reported are for plasma polymers made from fluorine-rich monomers or monomer mixtures and it has been suggested that the selectivity of plasma polymer films is related to the high affinity of oxygen to fluorine-containing compounds.<sup>2,5</sup> In this work we examined the transport of several simple gases through plasma polymer films made from a microwave discharge of benzene, mono-, di-, tri-, and perfluorobenzene, pentafluorotoluene, pentafluoropyridine, and perfluoromethylcyclohexane. In this group of monomers the  $F/C$  ratio varies from 0 to 2 and allows us to examine the effect of the fluorine to carbon

ratio of the monomer on the permselectivity of the resulting plasma polymer films. To more fully characterize the permeation properties of the plasma polymer films, we also measured the permeation of several different permeant gases that were chosen to span a range of kinetic diameters.

## EXPERIMENTAL

### Monomers

The monomers used in this work were benzene, monofluorobenzene, 1,2-difluorobenzene, 1,2,4-trifluorobenzene, pentafluorobenzene, hexafluorobenzene, pentafluoropyridine, pentafluorotoluene, and perfluoromethylcyclohexane. All monomers were purchased from Aldrich and were used without further purification. At the beginning of a set of plasma depositions, the monomer reservoir is connected to the system and the entire system is degassed for 15 min by pumping with all valves wide open.

### Plasma Polymerization

Plasma polymer films were produced in a microwave (2.45 GHz) powered plasma reactor. A schematic of the system is shown in Figure 1. The reaction chamber is a 35-mm o.d. Pyrex tube sealed at one end. The open end of the tube is connected to a vacuum pump (Alcatel 2012 cp) through a throttle valve and

\* To whom correspondence should be addressed.

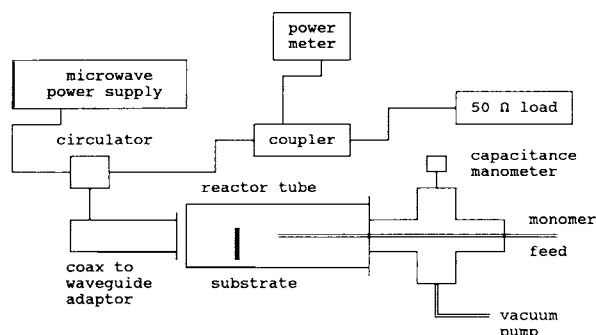


**Figure 1** Schematic of the microwave plasma deposition system.

a shutoff valve. The monomers used for polymerization are introduced through a 6-mm Pyrex tube that enters the system as shown. The distance between the closed end of the large tube and the end of the monomer inlet tube is 15 cm. A coaxial cable connects the microwave power supply (Ophos Instruments, Rockville, MD) to a coax-to-wave guide adaptor. Power is coupled to the reactor tube through the open end of the wave guide that is placed against the sealed end of the large Pyrex tube. A circulator and a 50- $\Omega$  load are used to protect the power supply from reflected power. A thermistor (Hewlett-Packard 8478B) and power meter (Hewlett-Packard 432A) are used to measure the reflected power through a 20-dB directional coupler and a 20-dB attenuator. A power meter on the microwave supply indicates the incident power. A capacitance manometer is used to monitor the system pressure and to determine gas flow rates.

Initially, we were concerned that the open end of the wave guide would broadcast considerable microwave power. At our normal operating conditions

( $\sim 30$  W), leakage from this system is below 1 mW/cm<sup>2</sup> as determined using a microwave leakage detector (Simpson model 380). Microwave leakage can be further reduced by judicious placement of copper screens or Al foil, if needed. Reflected power is a function of the spacing between the open end of the wave guide and the tube and is generally less than 5% of the incident power.

The plasma polymer is deposited onto Celgard (Hoechst Celanese) substrates. Celgard is a porous polypropylene material (pore size = 0.05  $\mu$ m, porosity = 38%) that gives some strength to the resulting composite film; the Celgard itself is not permselective. The substrates are placed perpendicular to the axis of the reactor tube using a glass support  $\sim 6$  cm away from the closed end of the tube. A small magnet inside the glass support allows adjustment of the position of the substrate within the reactor tube.

The glowing region of the plasma is confined to the first 4 or 5 cm of the tube. The substrates are placed 1 cm outside the edge of the glow region. If the substrates are placed further into the glow region the Celgard begins to degrade. The operating conditions for each monomer are listed in Table I. Argon is added to the monomer flow in all depositions and is essential for keeping the microwave discharge stable, particularly with the monomers that have a high fluorine content. We performed a number of preliminary experiments using different conditions. Many of the films we produced were leaky (high gas permeation rates and low selectivity), probably due to cracks in the films. Thus, we did not attempt to keep the conditions the same for each monomer but chose conditions that consistently gave nonleaky films.

**Table I** Plasma Polymerization Conditions and Oxygen to Nitrogen Permselectivities

Monomer	Polymerization Conditions				
	Flow Rates (sccm)		Pressure (Torr)	Power (W)	O <sub>2</sub> /N <sub>2</sub> Selectivity
	Monomer	Argon			
Benzene	4.0	2.0	0.08	20	1.2
Monofluorobenzene	4.0	2.0	0.07	20	1.3
1,2-Difluorobenzene	4.0	2.0	0.08	30	2.5
1,2,4-Trifluorobenzene	4.0	2.0	0.10	30	2.3
Pentafluorobenzene	4.0	2.0	0.08	30	3.5
Perfluorobenzene	4.0	4.0	0.10	30	3.4
Pentafluoropyridine	2.0	2.0	0.08	30	4.1
Pentafluorotoluene	3.0	3.0	0.09	30	4.1
Perfluoromethylcyclohexane	4.0	2.0	0.09	70	1.9

## Permeation Measurements

A permeation cell, similar to that described by Koros et al.<sup>10</sup> was constructed and used for the permeation rate measurements. A schematic diagram of the permeation system is shown in Figure 2.

The permeation cell consists of two halves that are separated by the film under test. The composite membrane, approximately  $1.5 \times 1.5$  cm, is sealed with Al foil adhesive tape. A  $\frac{1}{8}$  in. diameter hole in the center of the foil is left open to allow permeation through a well-defined area. Both sides of the film are supported by metal screens. The sample is protected from any damage from the screens by placing filter papers between the sample and the screen. One side of the cell is designated as the upstream (high pressure) side and the other as the downstream (low pressure) side. The volume of the downstream side is  $24.7 \text{ cm}^3$  which is determined by a liquid filling method. The plasma polymer coated side of the Celgard is exposed to the high pressure side of the cell.

Once a sample is loaded into the cell, the cell is placed into the constant temperature bath at  $35^\circ\text{C}$  and both sides of the cell are evacuated below 0.1 Torr using a two-stage rotary pump for at least 2 h, typically overnight. At the beginning of the measurement the upstream side is filled with the penetrant gas and is maintained at a constant pressure between 12 and 15 psia. The downstream side is isolated from the pump and the increase in pressure of the downstream side is monitored using an MKS pressure transducer (model 128A, 0–10 Torr). The pressure in the downstream side is less than 2 Torr throughout the run so that the pressure difference across the membrane is assumed to be equal to the upstream pressure. Data are collected using a PC connected to the pressure transducer. The permeation rate is determined from the slope of the linear portion of the downstream pressure increase with

time and is converted to a permeability coefficient using the known area and the thickness of the sample. The data are corrected for the system leak rate, which is typically less than 2% of the permeation rate through the sample.

In the permeation measurement, the permeation rate (or flow rate) of gas  $i$  through the membrane,  $Q_i$  [ $\text{cm}^3(\text{STP})$ ], is determined from the linear pressure increase with time using the downstream system volume. The flux constant, or conductance, of gas  $i$ ,  $\langle P_i \rangle / \delta$ , is suitable for comparing the permeation of various gases through the membranes and is related to the measured permeation rate by equation 1.

$$\frac{\langle P_i \rangle}{\delta} = \frac{Q_i}{\Delta p_i A} \quad (1)$$

In eq. (1)  $A$  is the unmasked area of the sample,  $\Delta p_i$  is the pressure difference of gas  $i$  across the film (assumed equal to the upstream pressure),  $\langle P_i \rangle$  is the average permeability coefficient of gas  $i$  through the membrane, and  $\delta$  is the permeation thickness. Throughout this work the units of  $\langle P \rangle / \delta$  are  $\text{cm}^3(\text{STP}) \text{ cm}^{-2} \text{ s}^{-1} \text{ cm Hg}^{-1}$ .

The ideal selectivity,  $R(i/j)$ , of a film is simply defined as the ratio of the permeability coefficients of two gases through the same film. In our case, the permeation of a series of gases through the same samples was measured so that the film thickness did not vary when testing the different gases. Thus, the ideal selectivity can be obtained from a ratio of the permeation flux constants as shown in eq. (2).

$$R(i/j) = \frac{\langle P_i \rangle}{\langle P_j \rangle} = \frac{(\langle P_i \rangle / \delta)}{(\langle P_j \rangle / \delta)} \quad (2)$$

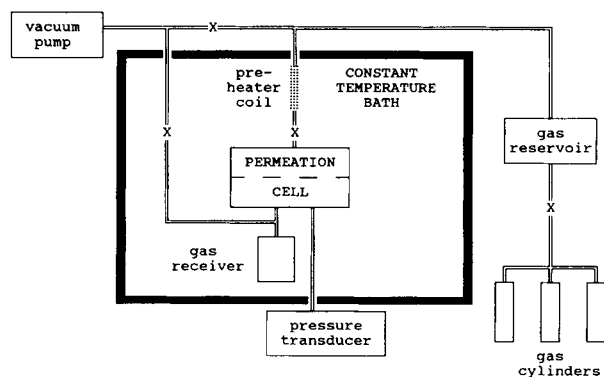


**Figure 2** Schematic of the permeation measurement system.

## Film Thickness

The nominal thickness of the plasma polymer films was determined by depositing plasma polymer films onto glass slides (instead of Celgard) under the same conditions as used to make the permeation samples. The thickness of the film on the glass substrate is measured using a Dektak IIA profilometer. Film thickness is uniform to within 15% across the sample. Most of the change in film thickness occurs at the edge of the sample. In the center of the samples, which is the portion used for the permeation tests, the thickness varies less than 2%. Deposition times for each monomer were adjusted so that the nominal thickness of our plasma polymer coatings is  $1.5 \mu\text{m}$ .

Ultimately, we would prefer to know the permeability coefficient rather than the conductance. In our membranes, which consist of a plasma polymer coating on a porous polymer support, it is impossible to be certain that the permeation thickness,  $\delta$ , is the same as the nominal thickness. In our discussion, we compare flux constants and ideal selectivities and do not report permeability coefficients except as noted later.

### Infrared Spectra

The plasma polymer samples were examined by infrared (IR) spectroscopy. To collect samples for IR, we routinely placed a glass slide adjacent to the Celgard substrate in the reactor. Plasma polymer film that deposited on the glass slide was scraped off, mullied with KBr, and pressed into pellets. The spectra were obtained using a BioRad FTS-60 Fourier transform IR spectrometer.

### Solubilities

Solubilities of  $\text{CO}_2$  and  $\text{CH}_4$  in the plasma polymers were obtained by measuring the weight gain of plasma polymer samples using a Cahn microbalance. The Cahn sorption apparatus is enclosed in a Pyrex chamber, which is enclosed in an insulated box. Approximately 200-mg samples of plasma polymer were obtained by collecting plasma polymer from several depositions (using the same deposition conditions). The polymer was placed into small Al foil cups that were hung from one arm of the balance in the Pyrex chamber. All measurements were made at  $35^\circ\text{C}$ . The chamber was evacuated and the weight of the sample recorded. The chamber was then filled with the sorption gas to a pressure of 1 atm and, after several hours of equilibration, the weight recorded again. The weight gain is corrected for buoyancy forces. The weight gains due to sorption of  $\text{O}_2$  and  $\text{N}_2$  were smaller than those due to the buoyancy effects; thus we could not reliably measure the solubility of these gases with our system.

## RESULTS

To obtain good selectivity data for plasma polymer films deposited onto porous substrates, it is necessary to deposit a thick enough layer of the plasma polymer to cover the pores in the substrate. Generally, it has been found that the thickness of the plasma polymer films must be 5–10 times the nominal pore size of the substrate to achieve selectiv-

ity.<sup>5,8,9</sup> For plasma polymer films thinner than this the films leak (i.e. they have high permeabilities) and show little or no permselectivity. Once the pores have been covered, the selectivity of the films increases and quickly reaches a plateau. We have found similar results with our plasma polymer films on Celgard substrates and use plasma polymer films with a nominal thickness of  $1.5\ \mu\text{m}$  in this work to ensure that the pores of the substrate are covered.

The deposition conditions and  $\text{O}_2/\text{N}_2$  selectivity values are listed in Table I for each of the monomers. The conditions listed in Table I were those that gave us the best results (nonleaky films) in our system. Heavier monomers generally required the use of higher power (or, in some cases, lower flow rates) as would be expected from a consideration of the composite power parameter,  $W/FM$  ( $W$  is the power,  $F$  is the monomer flow rate, and  $M$  is the monomer molecular weight), although we made no specific attempt to keep  $W/FM$  constant. The oxygen to nitrogen selectivity that we obtain for plasma films of perfluorobenzene (3.4) is less than the value of 4.5 reported by Terada et al.<sup>5</sup> and our value for perfluoromethylcyclohexane (1.9) is greater than the value of 1.1 reported by Inagaki and Kawai.<sup>2</sup> These differences are most likely due to different deposition conditions and different reactor geometries.

The IR spectra for benzene, monofluorobenzene, difluorobenzene, and pentafluorobenzene plasma polymer films are shown in Figure 3 and those of pentafluorotoluene, pentafluoropyridine, and hexafluorobenzene are shown in Figure 4. The plasma films from the low  $F/C$  ratio monomers have peaks at  $\sim 2800$  and  $1370\ \text{cm}^{-1}$ , which are due to  $\text{CH}_2$  and

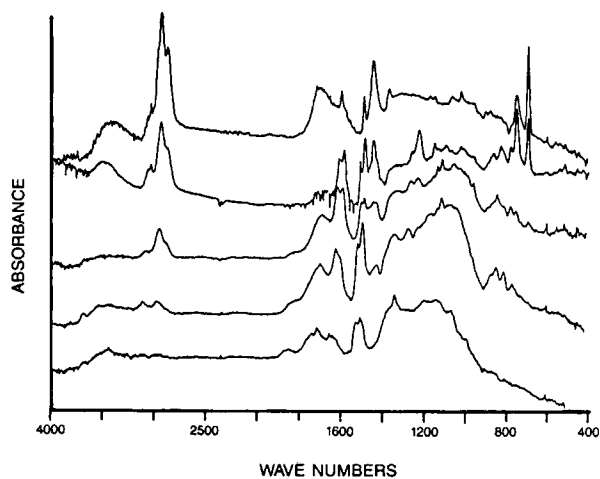


**Figure 3** Infrared spectra (top to bottom) of benzene, and mono-, di-, tri-, and pentafluorobenzene plasma polymers.

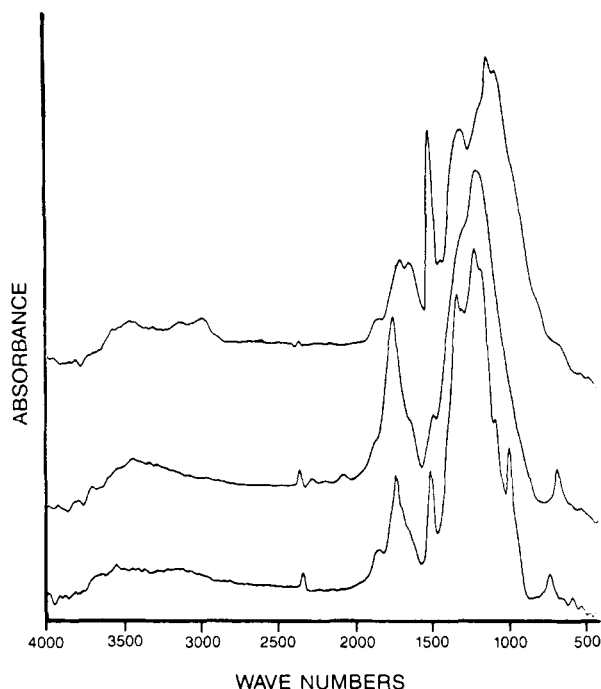


**Figure 4** Infrared spectra (top to bottom) of pentafluorotoluene, pentafluoropyridine, and hexafluorobenzene plasma polymers.

$\text{CH}_3$  groups. Aromaticity is retained in the polymers as is evident from the aromatic C-H absorption at  $3050\text{ cm}^{-1}$  and the aromatic C-C absorptions at  $1600$ ,  $1500$ , and  $1430\text{ cm}^{-1}$ . Benzene and monofluorobenzene plasma films also exhibit strong peaks at  $750$  and  $680\text{ cm}^{-1}$  that indicate monosubstituted (pendant) phenyl rings in the polymer. The plasma films resulting from the high F/C ratio monomers have little or no absorption in the region around  $3000\text{ cm}^{-1}$  as would be expected because there is little hydrogen in the monomer. The spectra of these polymers are dominated by absorption in the region between  $1200$  and  $1050\text{ cm}^{-1}$ . This broad absorption is a combination of contributions from fluorine-containing groups in different environments. Because the IR spectra of the low F/C and high F/C plasma films have very little in common, it is difficult to make qualitative comparisons. It is clear, however, that as the fluorine content of the monomer increases, the resulting plasma film has a greater fluorine content as would be expected based upon the composition of the monomers.

Shown in Figure 5 are the oxygen to nitrogen selectivities of the plasma films as a function of the F/C ratio of the monomers. With the aromatic monomers, a higher fluorine content in the monomer tends to yield more selective films and there is a more or less linear correlation between oxygen to

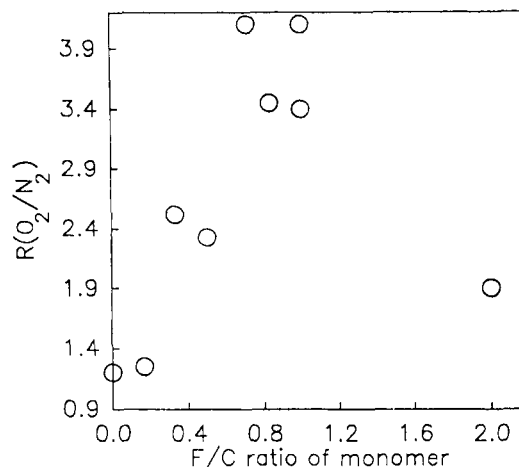


**Figure 5** Oxygen to nitrogen selectivity of the plasma films as a function of the F/C ratio of the monomer; data from Table I.

nitrogen selectivity and the F/C ratio of the monomer. This trend is not followed for perfluoromethylcyclohexane (F/C = 2), which of course is not aromatic.

In Figures 6 and 7 we show the permeation flux constants of these plasma films as a function of the kinetic diameter of the permeant gas. The plasma films that have a high oxygen to nitrogen selectivity (Fig. 6, perfluorobenzene, pentafluorotoluene, and pentafluoropyridine) all show similar gas permeation behavior. There is a general trend that the flux constant decreases as the kinetic diameter of the permeant gas increases. Benzene and monofluoroben-

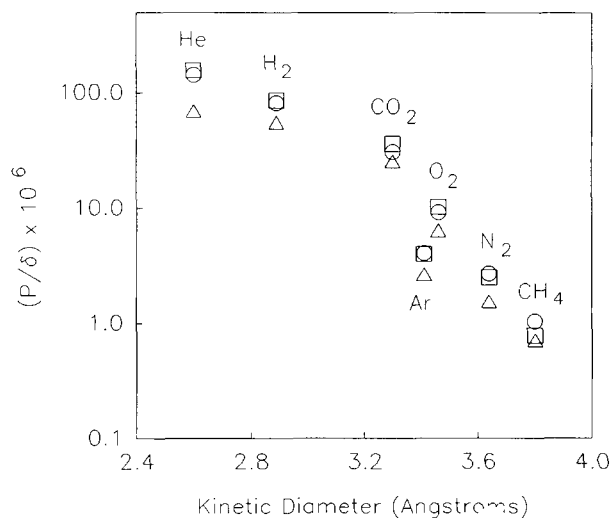


**Figure 6** Permeation flux constants (conductances) [ $\text{cm}^3(\text{STP})\text{ cm}^{-2}\text{ s}^{-1}\text{ cm Hg}^{-1}$ ] of simple gases in high permselectivity plasma polymer films: (□) perfluorobenzene, (Δ) pentafluorotoluene, and (○) pentafluoropyridine.

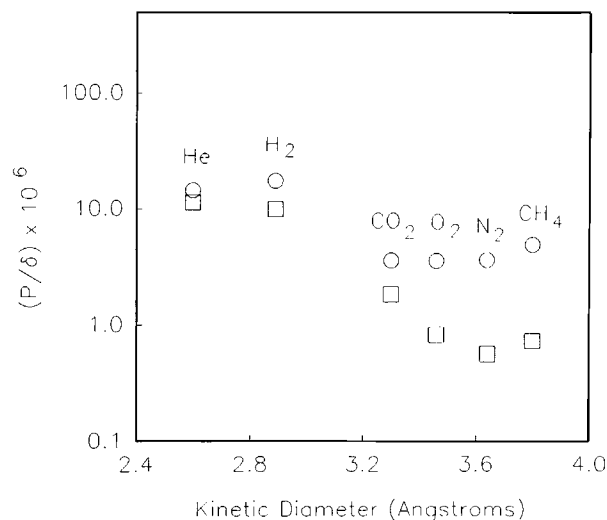


**Figure 7** Permeation flux constants (conductances) [ $\text{cm}^3(\text{STP}) \text{cm}^{-2} \text{s}^{-1} \text{cm Hg}^{-1}$ ] of simple gases in low permselectivity films: (O) benzene and (□) monofluorobenzene.

zene derived plasma films, which are less permselective, do not follow this trend (see Fig. 7). The permselectivities of plasma films of perfluorobenzene, pentafluoropyridine, pentafluorotoluene, benzene, and monofluorobenzene for different gas pairs are listed in Table II.

The solubilities of  $\text{CO}_2$  and  $\text{CH}_4$  in the plasma polymer films of hexafluorobenzene, pentafluorotoluene, and pentafluoropyridine were measured at  $35^\circ\text{C}$  and 1 atm. The values obtained are  $2.2 \times 10^{-1}$  ( $\pm 5\%$ )  $\text{cm}^3(\text{STP}) \text{cm}^{-3} \text{cm Hg}^{-1}$  for  $\text{CO}_2$  and  $3 \times 10^{-2}$  ( $\pm 20\%$ )  $\text{cm}^3(\text{STP}) \text{cm}^{-3} \text{cm Hg}^{-1}$  for  $\text{CH}_4$  in all of these plasma polymers. Weight gains due to sorption were measured three times by alternately evacuating and refilling the chamber with the same gas, and the reported values are averages of all measurements. The error on the  $\text{CH}_4$  solubility is large because the weight gain due to sorption is only slightly larger than that due to buoyancy forces. Higher gas pressures would allow more precise determination of solubilities but our system is not equipped to han-

dle pressures in excess of 1 atm. Terada et al.<sup>5</sup> reported solubilities of  $\text{O}_2$  and  $\text{N}_2$  in hexafluorobenzene plasma polymers and obtained (approximately)  $1 \times 10^{-2} \text{cm}^3(\text{STP}) \text{cm}^{-3} \text{cm Hg}^{-1}$ . We were not able to measure  $\text{O}_2$  and  $\text{N}_2$  solubilities in our system.

## DISCUSSION

As pointed out in the previous section, plasma films from benzene and the fluorobenzenes show a more or less linear correlation between the oxygen to nitrogen selectivity and the F/C ratio of the monomer (see Fig. 5). The IR results confirm that there is an increase in the fluorine content of the plasma polymers with an increase in F/C ratio of the monomers.

There are two possible explanations for the observed increase in  $\text{O}_2/\text{N}_2$  permselectivity with increasing fluorine content of the monomer. First, the solubility of oxygen in the plasma films increases with increasing fluorine content. Second, the structure of the plasma polymer changes with increasing fluorine content of the aromatic monomers making the plasma film more selective.

The first of these has been suggested by several authors who have stated that fluorine-containing monomers were chosen for study because the monomers have a "high affinity" for oxygen.<sup>2,5</sup> Presumably, this leads to plasma polymers that have a relatively high permeation rate for oxygen. In general, the solubility of oxygen in liquid fluorobenzenes does increase with the degree of fluorination of the benzene ring and so we might expect that these monomers would lead to plasma polymers that have high oxygen permeabilities. For example, the solubilities (mole fractions) of oxygen in benzene and perfluorobenzene are  $8.1 \times 10^{-4}$  and  $25.4 \times 10^{-4}$ ,<sup>11</sup> respectively. However, the solubilities of nitrogen in these same monomers are  $4.46 \times 10^{-4}$  and  $17.9 \times 10^{-4}$ .<sup>11</sup> Nitrogen solubility increases by a factor of 4 and oxygen solubility increases by only a factor of 3 between benzene and hexafluorobenzene. Based upon

**Table II** Permselectivities of Plasma Polymers Films from Various Monomers

Monomer	Permselectivity $R(i/j) = P_i/P_j$				
	$\text{O}_2/\text{N}_2$	$\text{He}/\text{CH}_4$	$\text{H}_2/\text{CH}_4$	$\text{CO}_2/\text{CH}_4$	$\text{N}_2/\text{CH}_4$
Benzene	1.2	3.0	3.6	0.73	0.74
Monofluorobenzene	1.3	15	14	2.5	0.77
Pentafluorotoluene	4.1	78	91	36	2.2
Pentafluoropyridine	4.1	110	200	46.2	3.4
Hexafluorobenzene	3.4	79	137	30	2.6

the solubilities of oxygen and nitrogen in the monomers, we would expect a decrease, rather than an increase, in the permselectivity of the resulting plasma polymer films with increasing fluorine content of the monomer.

We also found that the higher permselectivity of the plasma polymer films derived from high fluorine content monomers is not peculiar to oxygen and nitrogen. The data in Table II show that the plasma films that have higher oxygen to nitrogen permselectivities are also more selective for other gas pairs. Thus, it does not appear that any specific interactions between oxygen and the plasma polymer films are responsible for the higher selectivities observed. The higher selectivities of the plasma polymers derived from high fluorine content monomers is probably related to parameters such as the plasma polymer density and crosslink density. It is not clear, *a priori*, that an increased fluorine content of the monomer should lead to films with higher selectivity but the data presented in Table II seem to indicate that this is true.

The data presented in Figure 6 seem to indicate that the size of the permeant molecule is of primary importance in determining the flux constants, and selectivities, of the different gases through the plasma polymer films. Although it is generally true that small molecules, such as H<sub>2</sub> and He, will permeate faster than larger molecules, such as CH<sub>4</sub>, we should not conclude that size alone determines the permeation properties of a given permeant gas.

In the case of argon and oxygen, the kinetic diameters are very similar (3.41 and 3.46 Å, respectively) but their flux constants are  $4.0 \times 10^{-6}$  and  $10.2 \times 10^{-6}$  in pentafluoropyridine plasma polymers and  $2.7 \times 10^{-6}$  and  $6.4 \times 10^{-6}$  in pentafluorotoluene plasma polymers. Inagaki and Kawai<sup>2</sup> obtained similar results for oxygen and argon permeation through perfluoromethylcyclohexane/CH<sub>4</sub> plasma polymer films. In their work they found the ideal oxygen to nitrogen selectivity to be 2.4 whereas for argon and nitrogen the ideal selectivity is only 1.1. Because the kinetic diameters of oxygen and argon differ by only 1.5%, the large difference in permeation flux constants and selectivities relative to N<sub>2</sub> must be attributed to other factors, perhaps differences in solubility of these gases in the plasma polymer membranes. Unfortunately, we could not measure solubilities of any of these gases in our plasma polymer samples. Although Terada et al.<sup>5</sup> report solubility data for O<sub>2</sub> and N<sub>2</sub> in perfluorobenzene derived plasma polymers, we are not aware of any data on Ar.

Carbon dioxide presents additional, and perhaps more compelling, difficulties in attempting to correlate permeation properties with the size of the permeant gas. In constructing Figure 6 we used the collision diameter as our permeant size scale. Another commonly used size scale is the van der Waals radius. If we had used the van der Waals radius instead of the collision diameter, the relative positions of most of the data points in Figure 6 would remain unchanged except for CO<sub>2</sub>. The van der Waals radius of CO<sub>2</sub> is larger than that of CH<sub>4</sub> that would shift the CO<sub>2</sub> point to the right of the CH<sub>4</sub> point in the figure. Using the van der Waals radii would not give the same apparent correlation between permeation flux constant and size.

The solubility of CO<sub>2</sub> in our plasma polymer films is also quite large compared to the solubility of other gases into these, and similar, plasma polymer materials. The value that we obtain for CO<sub>2</sub> ( $2.2 \times 10^{-1}$  cm<sup>3</sup>(STP) cm<sup>-3</sup> cm Hg<sup>-1</sup>) is a factor of 7 larger than the value we obtain for CH<sub>4</sub> ( $3.0 \times 10^{-2}$  cm<sup>3</sup>(STP) cm<sup>-3</sup> cm Hg<sup>-1</sup>) and a factor of 20 larger than the value reported by Terada et al.<sup>5</sup> for the solubilities of O<sub>2</sub> and N<sub>2</sub> in hexafluorobenzene plasma polymer films. For comparison, the solubility of CO<sub>2</sub> in FEP [hexafluoropropylene/poly(tetrafluoroethylene) copolymer]<sup>12</sup> is only a factor of 4 greater than that O<sub>2</sub>, a factor of 7 greater than that of N<sub>2</sub>, and a factor of 4 greater than that of CH<sub>4</sub>. The relatively high solubility of CO<sub>2</sub> in our plasma polymer films contributes to the high value of the flux constant of CO<sub>2</sub> and the high CO<sub>2</sub>/CH<sub>4</sub> permselectivity in the plasma films of hexafluorobenzene, pentafluorotoluene, and pentafluoropyridine.

For O<sub>2</sub> and N<sub>2</sub> the ideal selectivity of our fluorine-rich plasma polymer films is much less than the ideal selectivity reported for polysulfones, the material used to make commercial membranes. For example, McHattie et al. report ideal oxygen to nitrogen selectivities between 5 and 7, depending upon the type of polysulfone.<sup>13</sup> For CO<sub>2</sub> and CH<sub>4</sub> these authors report ideal selectivities ranging from 22 to 34. The fluorine-rich plasma polymers yield ideal selectivities between 30 and 46. In Figure 8 we have plotted the ideal selectivities,  $R(\text{CO}_2/\text{CH}_4)$ , of our plasma polymer films and several conventional polymers (including polysulfone) as a function of the CO<sub>2</sub> permeability coefficient. For the purposes of this comparison, we have assumed that the thickness of the plasma polymer films on Celgard substrates are the same as those measured on glass substrates so that we could estimate the CO<sub>2</sub> permeability coefficients of our films. The plasma polymers produced from hexafluorobenzene, pentafluorotoluene, and

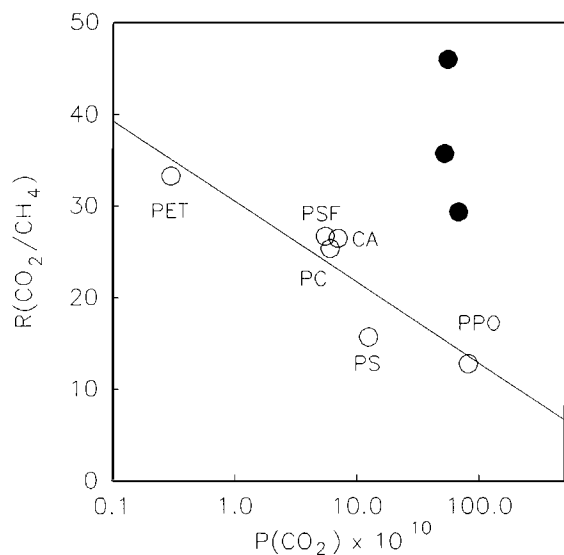


**Figure 8** Comparison of  $\text{CO}_2/\text{CH}_4$  selectivity of plasma polymer films with conventional polymers. The open circles correspond to conventional polymers: PET, poly(ethylene terephthalate)<sup>13</sup>; PSF, polysulfone<sup>14</sup>; CA, cellulose acetate<sup>15</sup>; PC, polycarbonate<sup>16</sup>; PS, polystyrene<sup>17</sup>; PPO, poly(phenylene oxide)<sup>18</sup>. The filled circles correspond to our plasma films of hexafluorobenzene, pentafluorotoluene, and pentafluoropyridine.

pentafluorotoluene yield membranes with both good selectivity and relatively high  $\text{CO}_2$  permeability coefficients.

## CONCLUSIONS

Permselective plasma films were produced by microwave discharge of fluorinated monomers. Fluorine-rich aromatic monomers, such as perfluorobenzene, pentafluoropyridine, and pentafluorotoluene, produce polymer films with the highest selectivities. In the case of  $\text{O}_2$  to  $\text{N}_2$  selectivity, there appears to be a correlation between selectivity and the fluorine to carbon ratio of the monomer. High selectivity, however, is not peculiar to  $\text{O}_2$  and  $\text{N}_2$ ; the films that exhibit  $\text{O}_2$  to  $\text{N}_2$  selectivity are also selective for other gas pairs. Thus, the selectivity of these films is likely due to the film structure rather

than to specific interactions between the plasma polymer and any of the permeant gases, except perhaps in the case of  $\text{CO}_2$ .  $\text{CO}_2$  has an anomalously high solubility in these plasma polymers that contributes to the high permeation flux constant and the high  $\text{CO}_2$  to  $\text{CH}_4$  selectivity in these membranes.

## REFERENCES

1. N. Inagaki and J. Ohkubo, *J. Membr. Sci.*, **27**, 63 (1986).
2. N. Inagaki and H. Kawai, *J. Polym. Sci. Part A: Polym. Chem.*, **24**, 3381 (1986).
3. N. Inagaki and H. Katsuoka, *J. Membr. Sci.* **34**, 297 (1987).
4. N. Inagaki, S. Tasaka, and M. Park, *J. Appl. Polym. Sci.*, **40**, 143 (1990).
5. I. Terada, T. Haraguchi, and T. Kajiyama, *Polym. J.*, **18**, 529 (1986).
6. H. Nomura, P. Kramer, and H. Yasuda, *Thin Solid Films*, **118**, 187 (1984).
7. M. Yamamoto, J. Sakata, and M. Hirai, *J. Appl. Polym. Sci.*, **29**, 2981 (1984).
8. J. Sakata, M. Yamamoto, and M. Hirai, *J. Appl. Polym. Sci.*, **31**, 1999 (1986).
9. J. Skata, M. Yamamoto, and M. Hirai, *J. Appl. Polym. Sci.*, **34**, 2701 (1987).
10. W. Koros, D. Paul, and A. Rocha, *J. Polym. Sci. Polym. Phys. Ed.*, **14**, 687 (1976).
11. M. Hamza and G. Serratrice, *J. Am. Chem. Soc.*, **103**, 3733 (1981).
12. R. A. Pasternak, G. L. Burns, and J. Heller, *Macromolecules*, **4**, 470 (1971).
13. J. S. McHattie, W. J. Koros, and D. R. Paul, *Polymer*, **32**, 840 (1991).
14. I. Cabasso, *Encyclopedia of Polymer Science and Engineering*, 2nd ed., Vol. 9, Wiley, New York, 1987.
15. N. Muruganandam, W. J. Koros, and D. R. Paul, *J. Polym. Sci. Polym. Phys. Ed.*, **25**, 1999 (1987).
16. A. C. Puleo, N. Muruganandam, and D. R. Paul, *J. Polym. Sci. Polym. Phys. Ed.*, **27**, 2385 (1989).
17. G. Perego, A. Roggero, R. Sisto, and C. Valentini, *J. Membr. Sci.*, **55**, 325 (1991).
18. S. A. Stern, Y. Mi, H. Yamamoto, and A. K. St. Clair, *J. Polym. Sci. Polym. Phys. Ed.*, **27**, 1887 (1989).

Received August 4, 1994

Accepted February 28, 1995